Cobaloximes with Mixed Dioximes of Glyoxime and Diphenylglyoxime: Synthesis, Characterization, CV, X-ray Studies, and Crystal Packing

B. D. Gupta,* R. Yamuna, and Debaprasad Mandal

Department of Chemistry, Indian Institute of Technology, Kanpur, India 208016

Received October 23, 2005

Fourteen complexes of inorganic and alkyl cobaloximes with mixed dioximes of the type (R/X)Co(gH)(dpgH)Py have been synthesized and characterized by ^{1}H and ^{13}C NMR and UV. The spectral data are interrelated, and a good correlation is found between $\Delta\delta^1$H(Py$_\alpha$) with δ^1H(gH), δ^{13}C(C═N$_{gH}$), and δ^{13}C(C═N$_{dpgH}$) indicating the ring current throughout the Co(dioxime)$_2^+$ metallabicycle. All the spectroscopic data and CV show dependence on the field effect. The X-ray structure and crystal packing in ClCo(gH)(dpgH)Py, C_2H_5Co(gH)(dpgH)Py, and C_8H_{17}Co(gH)(dpgH)Py have been studied. ClCo(gH)(dpgH)Py shows a right-handed helix.

Introduction

Cobaloximes,[1] proposed as model of B_{12} coenzyme about 4 decades ago, represent a unique class of compounds in organometallic and bioinorganic chemistry, and because of their rich coordination chemistry and potential applications in organic synthesis, they have now acquired an independent research field.[2]

Many papers have appeared in the recent past that describe the spectral and structural properties of cobaloximes. The reported trends are related to the mutual cis and trans influence of the ligands, as reflected in their NMR chemical shifts.[3−5] The studies describe the correlation of ^{1}H NMR chemical shifts of axial ligands B with those of the equatorial ligands and also include the multilinear correlation of ^{1}H NMR chemical shifts of B with the Co → dioxH charge-transfer band.[5] The spectral correlations initially were interpreted by Marzilli on the basis of cobalt anisotropy[3a−f,4c,6] and then by López on the basis of ring current formalism[5] and recently by us using the field effect (total effect of cobalt anisotropy and ring current).[7] Most of the information is on cobaloximes with dmgH as the equatorial ligand, and studies with other dioximes such as gH,[8a,b] chgH,[8c] dpgH,[8d,e] and dmestgH[7] are few. We have recently reported the synthesis and cis−trans influence studies in mixed dioxime cobaloximes.[9] Despite the reduced ring current and cobalt anisotropy in these complexes, the spectral data fitted well as per our model. The cis influence order was found to be dmestgH > dpgH > dmgH-dpgH > chgH-dpgH > dmgH > gH > chgH. The study on the gH complexes, however, was hampered

* To whom correspondence should be addressed. Tel: +91−512−2597046. Fax: +91−512−2597436. E-mail: bdg@iitk.ac.in.

(1) Cobaloximes have the general formula RCo(L)$_2$B, where R is an organic group σ-bonded to cobalt. B is an axial base trans to the organic group, and L is a monoanionic dioxime ligand (e.g. glyoxime (gH), dimethylglyoxime (dmgH), 1,2-cyclohexanedione dioxime (chgH), diphenylglyoxime (dpgH), and dimesitylglyoxime (dmestgH)).

(2) (a) Giese, B. *Radicals in Organic Synthesis: Formation of Carbon−Carbon Bonds*; Pergamon Press: Oxford, U.K., 1986. (b) Scheffold, R.; Rytez, G.; Walder, L. In *Transition Metals in Organic Synthesis*; Scheffold, S., Ed.; Wiley: Chichester, U.K., 1983; Vol. 3. (c) Branchaud, B. P.; Friestad, G. F. Vitamin B12. In *Encyclopedia of Reagents for Organic Synthesis*; Paquette, L. A., Ed.; Wiley: Chichester, U.K., 1995; p 5511. (d) Welker, M. E. *Curr. Org. Chem.* **2001**, *5*, 785. (e) Tada, M. *Rev. Heteroat. Chem.* **1999**, *20*, 97. (f) Nishikubo, Y. L.; Branchaud, B. P. *J. Am. Chem. Soc.* **1999**, *121*, 10924. (g) Tucker, C. J.; Welker, M. E. Day, C. S.; Wright, M. W. *Organometallics* **2004**, *23*, 2257. (h) Wright, M. W.; Welker, M. E. *J. Org. Chem.* **1996,** *61*, 133. (i) Brown, T.; Dronsfield, A.; Jablonski, A.; Wilkinson, A. S. *Tetrahedron Lett.* **1996**, *37*, 5413. (j) Gill, G. B.; Pattenden, G.; Roan, G. A. *Tetrahedron Lett.* **1996**, *37*, 9369. (k) Gupta, B. D.; Vijaikanth, V. *J. Organomet. Chem.* **2004**, *689*, 1102 and references therein. (l) Gridnev, A. A.; Ittel, S. D. *Chem. Rev.* **2001**, *101*, 3611. (m) Wright, M. W.; Smalley, T. L.; Welker, M. E.; Rheingold, A. L. *J. Am. Chem. Soc.* **1994**, *116*, 6777. (n) Smalley, T. L.; Wright, M. W.; Garmon, S. A.; Welker, M. E.; Rheingold, A. L. *Organometallics* **1993**, *12*, 998. (o) Branchaud, B. P.; Choi, Y. L. *Tetrahedron Lett.* **1988**, *29*, 6037.

(3) (a) Marzilli, L. G.; Bayo, F.; Summers, M. F.; Thomas, L. B.; Zangrando, E.; Bresciani-Pahor, N.; Mari, M.; Randaccio, L. *J. Am. Chem. Soc.* **1987**, *109*, 6045. (b) Brown, K. L.; Satyanarayana, S. *J. Am. Chem. Soc.* **1992**, *114*, 5674. (c) Zangrando, E.; Bresciani-Pahor, N.; Randaccio, L.; Charland, J. P.; Marzilli, L. G. *Organometallics* **1986**, *5*, 1938. (d) Bresciani-Pahor, N.; Geremia, S.; López, C.; Randaccio, L.; Zangrando, E. *Inorg. Chem.* **1990**, *29*, 1043. (e) Trogler, W. C.; Stewart, R. C.; Epps, L. A.; Marzilli, L. G. *Inorg. Chem.* **1974**, *13*, 1564. (f) Randaccio, L.; Geremia, S.; Zangrando, E.; Ebert, C. *Inorg. Chem.* **1994**, *33*, 4641. (g) Stewart, R. C.; Marzilli, L. G. *Inorg. Chem.* **1977**, *16*, 424. (h) Hamza, M. S. A.; Felluga, A.; Randaccio, L.; Tauzher, G.; van Eldik, R. *Dalton Trans.* **2004**, 287.

(4) (a) Brown, K. L.; Lyles, D.; Penencovici, M.; Kallen, R. G. *J. Am. Chem. Soc.* **1975**, *97*, 7338. (b) Randaccio, L.; Bresciani-Pahor, N.; Toscano, P. J.; Marzilli, L. G. *J. Am. Chem. Soc.* **1981**, *103*, 6347. (c) Charland, J. P.; Zangrando, E.; Bresciani-Pahor, N.; Randaccio, L. Marzilli, L. G. *Inorg. Chem.* **1993**, *32*, 4256. (d) Cini, R.; Moore, S. J.; Marzilli, L. G. *Inorg. Chem.* **1998**, *37*, 6890. (e) Bresciani-Pahor, N.; Randaccio, L.; Zangrando, E.; Summers, M. F., Jr.; Ramsden, J. H.; Marzilli, P. A.; Marzilli, L. G. *Orgnometallics* **1985**, *4*, 2086. (f) Toscano, P. J.; Swider, T. F.; Marzilli, L. G. Bresciani-Pahor, N.; Randaccio, L. *Inorg. Chem.* **1983**, *22*, 3416. (g) Drago, R. S. *Inorg. Chem.* **1995**, *34*, 3543. (h) Drago, R. S. *J. Organomet. Chem.* **1996**, *512*, 61.

(5) (a) López, C.; Alvarez, S.; Solans, X.; Font-Altaba, M. *Inorg. Chem.* **1986**, *25*, 2962. (b) López, C.; Alvarez, S.; Solans, X.; Font-Altaba, M. *Inorg. Chim. Acta* **1986**, *111*, L19. (c) Gilaberte, J. M.; López, C.; Alvarez, S.; Font-Bardia, M.; Solans, X. *New J. Chem.* **1993**, *17*, 193. (d) Gilaberte, J. M.; López, C.; Alvarez, S. *J. Organomet. Chem.* **1988**, *342*, C13.

(6) Moore, S. J.; Marzilli, L. G. *Inorg. Chem.* **1998**, *37*, 5329.

(7) Mandal, D.; Gupta, B. D. *Organometallics* **2005**, *24*, 1501.

(8) (a) Gupta, B. D.; Yamuna, R.; Singh, V.; Tewari, U. *Orgnometallics* **2003**, *22*, 226 and references therein. (b) López, C.; Alvarez, S.; Solans, X.; Font-Altaba, M. *Inorg. Chim. Acta* **1986**, *121*, 71. (c) Gupta, B. D.; Qanungo, K.; Yamuna, R.; Pandey, A.; Tewari, U.; Singh, V.; Vijaikanth, V.; Barclay, T.; Cordes, W. *J. Organomet. Chem.* **2000**, *608*, 106. (d) López, C.; Alvarez, S.; Font-Bardia, M. Solans, X. *J. Organomet. Chem.* **1991**, *414*, 245. (e) Toscano, P. J.; Lettko, L.; Schermerhorn, E. J.; Waechter, J.; Shufon, K.; Liu, S.; Dikarev, E. V.; Zubieta, J. *Polyhedron* **2003**, *22*, 2809.

(9) (a) Gupta, B. D.; Singh, V.; Yamuna, R.; Barclay, T.; Cordes, W. *Organometallics* **2003**, *22*, 2670. (b) Gupta, B. D.; Yamuna, R.; Singh, V.; Tewari, U.; Barclay, T.; Cordes, W. *J. Organomet. Chem.* **2001**, *627*, 80.

10.1021/om050919x CCC: $33.50
Publication on Web 12/30/2005

Chart 1

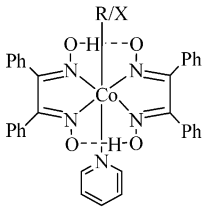

X = Cl, Br, NO_2, N_3 (**1a-4a**)

R = Me-Dec (**5a-14a**)

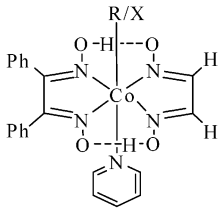

X = Cl, Br, NO_2, N_3 (**1b-4b**)

R = Me-Dec (**5b-14b**)

because of their poor solubility in common organic solvents.[8a] This problem has been alleviated in the present gH/dpgH systems.

There have only been a few reports on the electrochemical studies in cobaloximes. Recent work has indicated that the reduction potentials depend on both the axial and equatorial ligands.[7,8a,10] If this is so, then the CV data in the present mixed dioxime complexes should complement the existing view. We describe the first report of a CV study on the mixed dioxime complexes.

Despite the large number of crystal structure studies of cobaloximes and their related compounds, very little is known about the C−H···O, C−H···π intermolecular hydrogen-bonding interactions in the solid state leading to novel supramolecular structures.[9a,10a,11] Although the importance of weak hydrogen bonds in organic and biological systems has been successfully and forcefully elaborated in recent years, including its application in crystal engineering leading to the assembly of porous solids,[12] its application to inorganic and organometallic compounds has been limited only to a few systems.[13]

The aim of the present study is (a) to verify the validity of our recently proposed model for the interpretation of spectral correlations in mixed dioxime complexes, (b) to see if the data from different spectral studies such as ^{1}H, ^{13}C, UV−vis, and CV are interrelated, and (c) to look for supramolecular structures resulting from C−H···O, C−H···π, and π···π intermolecular bonding interactions in the solid state.

In this paper we report the synthesis and cis−trans influence study by ^{1}H, ^{13}C, UV−vis, and X-ray in (R/X)Co(gH)(dpgH)Py (R = Me−Dec and X = Cl, Br, NO_2, N_3). The X-ray structures of chloro, methyl, and octyl complexes are reported.

Experimental Section

^{1}H and ^{13}C NMR spectra were recorded on a JEOL JNM LAMBDA 400 FT NMR spectrometer (at 400 MHz for ^{1}H and 100 MHz for ^{13}C) in $CDCl_3$ solution with TMS as internal standard. NMR data are reported in ppm. UV−vis spectra were recorded in methanol on a Shimadzu 160A spectrometer. The degassed solvent was used for recording spectra. Elemental analyses were carried out at the Regional Sophisticated Instrumentation Center, Lucknow. A Julabo UC-20 low-temperature refrigerated circulator was used to maintain the desired temperature. Cyclic voltammetry measurements were carried out using a BAS Epsilon electrochemical workstation with a platinum working electrode, Ag/AgCl reference electrode (3 M KCl), and a platinum-wire counter electrode. All the measurements were performed in 0.1 M ^{n}Bu$_4$NPF$_6$ in dichloromethane (dry) at a concentration of 1 mM of each complex. In addition, in a separate series of experiments, an internal reference system (ferrocene/ferrocenium ion) was used. Under the conditions used, the reversible Fc/Fc$^+$ potential occurred at 0.51 V vs Ag/AgCl electrode.

Glyoxime (*Caution!* glyoxime is highly flammable and explosive when dry) diphenylglyoxime, and alkyl halides were purchased from Aldrich and were used as received. Silica gel (100−200 mesh) and distilled solvents were used in all chromatographic separations.

Crystal Structure Determinations and Refinements. A red crystal of **1b** and orange crystals of **6b** and **12b** were obtained by slow evaporation of the solutions of complexes in methanol and hexane. Single-crystal X-ray data were collected using graphite-monochromated Mo Kα radiation (λ = 0.710 73 Å) at room temperature for **1b** and **12b** on Mercury CCD AFC8S and Enraf-Nonius CAD-4 diffractometers, respectively, and at 100 K for **6b** on the Enraf-Nonius instrument. The space group is $P2_1/c$ for the compounds **1b** and **6b** and $P\bar{1}$ for **12b.** The structures were solved by direct methods using SHELXS-97 and refined isotropically by full-matrix least squares methods on F^2, using the SHELXL-93 and the SHELXL-97 computer programs.[14] All non-hydrogen atoms were refined with anisotropic displacement parameters. The hydrogen atom positions or thermal parameters were not refined but were included in the structure factor calculations. Since the cell measurements were recorded at high temperature (293(2) K) for compound **12b**, the thermal factors are high due to the high thermal motion of the alkyl chain. The pertinent crystal data and refinement parameters are compiled in Table 1.

ClCo^{III}(gH)(dpgH)Py (1b). Glyoxime (1.0 g, 11 mmol) and diphenylglyoxime (2.4 g, 10 mmol) were added to a solution of cobalt chloride hexahydrate (2.4 g, 10 mmol) in 95% ethanol (100 mL) followed by pyridine (2.0 mL, 24 mmol). The mixture was vigorously aerated for 20 min with occasional swirling. Water (5 mL) was added, and the mixture was aerated for another 1.5 h. The residue obtained after evaporation of the solvent was extracted with chloroform, and the organic layer was dried over anhydrous sodium sulfate. The crude product obtained after evaporation of chloroform was column-chromatographed on silica gel (100−200 mesh). ClCo(dpgH)$_2$Py (0.631 g, 10%) elutes out first with 10% ethyl acetate in chloroform. This was followed by ClCo(gH)(dpgH)Py (2.927 g, 58%) when the polarity was increased to 50% ethyl acetate in chloroform. The corresponding gH complex was formed in trace quantities.

XCo^{III}(gH)(dpgH)Py (2b−4b). The complexes were synthesized by following the procedure detailed earlier for XCo^{III}(dioxime)(dpgH)Py (dioxime = dmgH, chgH). Two products were formed in each reaction, which were separated by column chromatography using silica gel with ethyl acetate/chloroform mixture as the eluent. N_3Co(dpgH)$_2$Py (0.032 g, 11%) elutes out first with 50% ethyl acetate, followed by N_3Co(gH)(dpgH)Py (0.115 g, 50%) when the polarity was increased to 90% ethyl acetate.

RCo^{III}(gH)(dpgH)Py (5b−14b): General Procedure. A solution of **1b** (0.200 g, 0.4 mmol) in methanol (10 mL) was thoroughly purged with argon and was cooled to 0 °C. The solution turned deep blue on addition of NaOH followed by $NaBH_4$ (0.026 g, dissolved in 0.5 mL of water). Alkyl halide (1.2 mmol, 3 equiv) in methanol (2 mL) was added dropwise. Acetic acid (2 mL) was

(10) (a) Gupta, B. D.; Vijaykanth, V.; Veena, S. *Organometallics* **2004**, *23*, 2069. (b) Asaro, F.; Dreos, R.; Nardin, G.; Pellizer, G.; Peressini, S.; Randaccio, L.; Siega, P.; Trauzher, G.; Tavagnacco, C. *J. Organomet. Chem.* **2000**, *601*, 114.

(11) (a) Zhang, X.; Song, X.-Y.; Li, Y.-Z.; Chen, H. L. *J. Mol. Struct.* **2005**, *749*, 1. (b) Giese, B.; Hartung, J.; Lindner, H.-J.; Svoboda, I.; Paulus, H. *Acta Crystallogr., Sect. C* **1995**, *51*, 2522.

(12) (a) Desiraju, G. R.; Steiner, T. *The Weak Hydrogen Bond in Structural Chemistry and Biology*; Oxford University Press: Oxford, U.K., 1999. (b) Braga, D.; Grepioni, F. *Acc. Chem. Res.* **2000**, *33*, 601. (c) Steiner, T. *Angew. Chem., Int. Ed.* **2002**, *41*, 48−76.

(13) (a) Beatty, A. M. *CrystEngComm* **2001**, 51. (b) Braga, D.; Maini, L.; Polito, M.; Scaccianoce, L.; Cojazzi, G.; Grepioni. F. *Coord. Chem. Rev.* **2001**, *216−217*, 225.

(14) (a) Sheldrick, G. M. SHELXL-93, Program for the Refinement of Crystal Structures; University of Göttingen, Göttingen, Germany, 1993. (b) Sheldrick, G. M. SHELXL-97, Program for Crystal Structure Analysis (release 97-2); University of Göttingen, Göttingen, Germany, 1998.

Table 1. Crystal Data and Structure Refinement Details for 1b, 6b, and 12b

	1b	6b	12b
empirical formula	$C_{21}H_{19}ClCoN_5O_4$	$C_{46}H_{48}Co_2N_{10}O_8$	$C_{29}H_{36}CoN_5O_4$
formula wt	499.79	986.80	577.56
temp (K)	293(2)	100(2)	293(2)
radiation, λ(Mo Kα) (Å)	0.710 73	0.710 73	0.710 73
cryst syst	monoclinic	monoclinic	triclinic
space group	$P2_1/c$	$P2_1/c$	$P\bar{1}$
unit cell dimens			
a (Å)	10.6124(6)	24.946(13)	11.076(5)
b (Å)	10.6725(10)	11.625(6)	12.299(5)
c (Å)	19.5201(4)	15.603(8)	12.299(5)
α (deg)	90	90	80.697(5)
β (deg)	98.8091(4)	101.14(10)	71.207(5)
γ (deg)	90	90	64.859(5)
V (Å^3)	2184.8(2)	4439.6(4)	1435.2(10)
Z; ρ (calcd) (Mg/m^3)	4; 1.519	4; 1.476	2; 1.336
μ (mm^{-1})	0.946	0.814	0.640
F(000)	1024	2048	608
cryst size (mm^3)	0.34 × 0.16 × 0.16	0.29 × 0.20 × 0.18	0.20 × 0.10 × 0.10
index ranges	$-14 \le h \le 14$	$-33 \le h \le 33$	$0 \le h \le 11$
	$-14 \le k \le 14$	$-15 \le k \le 9$	$-13 \le k \le 13$
	$-26 \le l \le 26$	$-18 \le l \le 20$	$-13 \le l \le 13$
no. of rflns collected/unique	5349/5348 (R(int) = 0.036)	28 839/10 946 (R(int) = 0.0323)	5136/4849 (R(int) = 0.0865)
refinement method	full-matrix least squares on F^2	full-matrix least squares on F^2	full-matrix least squares on F^2
goodness of fit on F^2	1.076	1.030	1.009
final R indices ($I > 2\sigma(I)$)	R1 = 0.0439, wR2 = 0.1155	R1 = 0.0451, wR2 = 0.1054	R1 = 0.0727, wR2 = 0.1612
R indices (all data)	R1 = 0.0811, wR2 = 0.1314	R1 = 0.0557, wR2 = 0.1107	R1 = 0.1470, wR2 = 0.1985
no. of data/restraints/params	5348/0/365	10 946/0/679	4849/0/353

Table 2. Elemental Analysis Data, R_f Values, λ_{max} Values (nm), and Yields (%) for 1b−14b

		anal. found (calcd)					
no.	formula	C	H	N	R_f[a]	λ_{max} (log ϵ)[b]	yield (%)
1b	$C_{21}H_{19}ClCoN_5O_4$	50.73 (50.46)	3.75 (3.83)	14.16 (14.01)	0.63	245.2 (3.62)	58
2b	$C_{21}H_{19}BrCoN_5O_4$	46.10 (46.34)	3.48 (3.52)	12.95 (12.87)	0.63	251.2 (3.60)	36
3b	$C_{21}H_{19}CoN_6O_6$	49.64 (49.42)	3.78 (3.75)	16.38 (16.47)	0.59	258.2 (3.57)	37
4b	$C_{21}H_{19}CoN_8O_4$	50.05 (49.81)	3.76 (3.78)	22.02 (22.13)	0.65	254.8 (3.77)	50
5b	$C_{22}H_{22}CoN_5O_4$	54.76 (55.12)	4.67 (4.63)	14.49 (14.61)	0.73	393.0 (3.52), 234 (4.60)	29
6b	$C_{23}H_{24}CoN_5O_4$	55.79 (55.99)	4.88 (4.90)	14.11 (14.19)	0.72	462.5 (3.43), 236.0 (4.49)	27
7b	$C_{24}H_{26}CoN_5O_4$	57.17 (56.81)	5.17 (5.16)	13.67 (13.80)	0.72	461.4 (3.49), 234.0 (4.64)	31
8b	$C_{25}H_{28}CoN_5O_4$	57.10 (57.58)	5.46 (5.41)	13.47 (13.43)	0.72	463.2 (3.35), 235.0 (4.45)	39
9b	$C_{26}H_{30}CoN_5O_4$	58.39 (58.32)	5.59 (5.65)	13.14 (13.08)	0.72	462.5 (3.30), 235.0 (4.39)	31
10b	$C_{27}H_{32}CoN_5O_4$	59.62 (59.01)	5.89 (5.87)	12.63 (12.74)	0.74	461.9 (3.34), 237.5 (4.40)	29
11b	$C_{28}H_{34}CoN_5O_4$	59.29 (59.68)	6.10 (6.08)	12.50 (12.43)	0.73	462.4 (3.18), 235.0 (4.28)	26
12b	$C_{29}H_{36}CoN_5O_4$	59.93 (60.31)	6.31 (6.28)	12.07 (12.13)	0.73	463.1 (3.41), 234.0 (4.50)	34
13b	$C_{30}H_{38}CoN_5O_4$	61.22 (60.91)	6.44 (6.47)	11.79 (11.84)	0.75	463.3 (3.39), 236.0 (4.48)	32
14b	$C_{31}H_{40}CoN_5O_4$	61.19 (61.48)	6.70 (6.66)	11.61 (11.56)	0.77	463.4 (3.43), 235.0 (4.50)	25

[a] 100% ethyl acetate. [b] Methanol as solvent.

added to the reaction vessel after 45 min. The reaction mixture was stirred for 1 h in the dark, during which time it was brought to ambient temperature and the contents were poured into cold water. The orange-red solid was filtered and dried and on chromatographic separation gave two products, $RCo(dpgH)_2Py$ (10−15%) and RCo(gH)(dpgH)Py (49−57%). The dpgH complex eluted out first with 10% ethyl acetate in chloroform, followed by the mixed dioxime complex (**5b**−**14b**) with a 40−60% ethyl acetate/chloroform mixture. Any deviation in the solvent ratio gave contaminated products.

Results and Discussion

Synthesis. The mixed dioxime cobaloximes were unknown till recently. We have reported the synthesis of (R/X)Co(dioxime)(dpgH)Py, where dioxime = dmgH, chgH, R = benzyl, alkyl, and X = Cl, Br, NO_2, N_3,[9,15] and proposed a reaction scheme based on independent reactions. We have, therefore, made no attempt to study the mechanism in the present systems.

The complexes **2b**−**4b** are synthesized by the nucleophilic substitution of the chloro group in **1b**. The oxidative alkylation of Co^{I}(gH)(dpgH)Py with alkyl halide forms two products, $RCo^{III}(dpgH)_2Py$ (**5a**−**14a**) and RCo^{III}(gH)(dpgH)Py (**5b**−**14b**), the latter being the major product. This is in contrast to earlier studies where three products were formed.[9,15] The elemental analysis, UV−vis data, and R_f values of the compounds **1b**−**14b** are given in Table 2.

Spectroscopy. (a) ^{1}H and ^{13}C NMR Assignments. ^{1}H and ^{13}C resonances of dpgH, Co−CH_2, and Py_β are easily assigned on the basis of their chemical shifts. The assignments are consistent with the related and previously described cobaloximes (R/X)Co(dioxime)$_2$Py and (R/X)Co(dioxime)(dpgH)Py.[8a,16,17] ^{1}H and ^{13}C values for complexes **1b**−**14b** are given in Tables 3 and 4, respectively. Since $\delta^{13}C(C{=}N_{dpgH})$, $\delta^{13}C(Py_\alpha)$ and $\delta^{13}C(Py_\gamma)$, and $\delta^{13}C(C{=}N_{gH})$ occur very close to each other, their assignment has been confirmed by ^{1}H−^{13}C correlation experiments (Supporting Information).

(15) Gupta, B. D.; Tiwari, U.; Barclay, T.; Cordes, W. *J. Organomet. Chem.* **2001**, *629*, 83.

(16) Gupta, B. D.; Kushal, Q. *J. Organomet. Chem.* **1997**, *543*, 125.

(17) Gupta, B. D.; Kushal, Q. Barclay, T.; Cordes, W. *J. Organomet. Chem.* **1998**, *560*, 155.

Table 3. ^{1}H NMR Data (ppm) for 1b−14b

	pyridine								
no.	α	β	γ	gH	CH_2−Co	rest of alkyl chain	Me	O−H···O	dpgH
1b	8.41	7.34	7.81	7.65				18.14	7.20 (d), 7.25−7.31
2b	8.41	7.36	7.81	7.66				18.14	7.17−7.21, 7.25−7.33
3b	8.46	7.38	7.84	7.66				17.97	7.16 (d), 7.25−7.34
4b	8.44	7.36	7.82	7.63				18.04	7.22−7.29
5b	8.77	7.43	7.83	7.47			1.24	18.33	7.07−7.10, 7.15−7.30
6b	8.76	7.42	7.81	7.47	2.12		0.69	18.27	7.07−7.09, 7.20−7.24
7b	8.76	7.41	7.81	7.47	2.00	1.26−1.35	0.92	18.17	7.07 (d), 7.23 (d)
8b	8.76	7.41	7.81	7.47	2.01	1.23−1.37	0.88	18.29	7.07 (d), 7.20−7.28
9b	8.76	7.41	7.81	7.47	2.01	1.26−1.31	0.85	18.30	7.07 (d), 7.21−7.24
10b	8.77	7.41	7.81	7.47	2.01	1.27−1.31	0.86	18.28	7.07 (d), 7.21−7.27
11b	8.76	7.41	7.81	7.47	2.02	1.24−1.30	0.85	18.24	7.06 (d), 7.20−7.24
12b	8.76	7.41	7.81	7.47	2.02	1.23−1.30	0.86	18.26	7.07 (d), 7.20−7.24
13b	8.76	7.41	7.81	7.47	2.02	1.23−1.30	0.86	18.28	7.07 (d), 7.20−7.30
14b	8.76	7.41	7.81	7.47	2.02	1.23−1.30	0.87	18.29	7.07 (d), 7.21−7.29

Table 4. ^{13}C NMR of 1b−14b

		pyridine					
no.	$C{=}N_{dpgH/gH}$	α	β	γ	CH_2−Co	rest of alkyl chain	dpgH
1b	154.02, 140.28	150.82	126.15	139.54			129.23, 129.63, 127.95, 129.81
2b	154.56, 140.72	150.54	126.16	139.44			129.43, 129.65, 128.01, 129.84
3b	153.99, 140.33	150.35	126.14	139.57			128.86, 129.51, 128.02, 129.97
4b	153.87, 139.81	150.98	126.22	139.50			129.03, 129.87, 128.01
5b	151.21, 137.73	149.85	125.62	138.05			129.65, 129.48, 127.89, 129.13
6b	151.22, 137.82	149.81	125.60	138.04	28.83	15.92	129.73, 129.42, 127.91, 129.10
7b	151.33, 137.85	149.85	125.57	137.96	29.68	23.92, 14.93	129.75, 129.47, 127.92, 129.13
8b	151.28, 137.81	149.86	125.57	137.96	34.67	33.00, 23.71, 13.99	129.78, 129.44, 127.94, 129.11
9b	151.26, 137.80	149.86	125.57	137.94	34.93	32.89, 30.32, 22.49, 4.13	129.79, 129.43, 127.93, 129.10
10b	151.27, 137.79	149.87	125.56	137.94	35.05	31.68, 30.65, 30.38, 2.69, 14.08	129.81, 129.44, 127.93, 129.10
11b	151.26, 137.80	149.89	125.57	137.94	35.05	31.91, 30.72, 30.67, 29.15, 22.64, 14.13	129.79, 129.44, 127.93, 129.11
12b	151.26, 137.79	149.87	125.57	137.94	35.08	31.86, 30.71, 30.68, 29.43, 29.33, 22.68, 14.12	129.81, 129.44, 127.93, 129.10
13b	151.26, 137.80	149.86	125.56	137.94	35.06	31.91, 30.69, 29.62, 29.47, 29.30, 22.67	129.79, 129.44, 127.92, 129.10
14b	151.26, 137.80	149.86	125.57	137.95	35.07	31.91, 30.68, 29.68, 29.60, 29.47, 29.36, 22.69, 14.13	129.78, 129.44, 127.93, 129.11

(b) Cis and Trans Influence Studies. The Co−C bond stability in cobaloximes depends on both the cis and trans influence. The former has gained importance only recently.[7,8a,c,9a,15−17] To study the cis influence, either the axial ligand R/X or base B is varied, keeping the same dioxime, or the dioxime is varied, keeping the axial ligands constant. The changes are then monitored spectroscopically. We have considered the chemical shifts of O−H···O, $C{=}N_{oximinic}$, and Py_α, since these were found to be most effected in earlier studies.[7,16]

δ(O−H···O) values in **5b**−**14b** lie between those of their parent cobaloximes, $RCo(dpgH)_2Py$[16] and $RCo(gH)_2Py$,[8a] and these appear consistently upfield as compared to the value in RCo(dmgH)(dpgH)Py.[9a] Overall, the O−H···O resonance follows the order dmestgH > dpgH > dmgH-dpgH > gH-dpgH > chgH-dpgH ≈ dmgH > gH > chgH.[7,8a,9a,16] δ(O−H···O) values in **1b**−**4b** always appear upfield by about 0.2−0.3 ppm as compared to those in **5b**−**14b** because of the higher cis influence of X on O−H···O.

$\delta^{13}C(C{=}N_{gH\ or\ dpgH})$ values always occur upfield in these complexes, as compared to those for the corresponding free ligand. The field effect in the metallabicycle for different dioximes (keeping R/X constant) can be understood by comparing the coordination shift, $\Delta\delta^{13}C(C{=}N)$.[18] $\Delta\delta^{13}C(C{=}N_{gH})$ in **1b**−**8b** is much higher (4−7 ppm) as compared to the corresponding value $\Delta\delta^{13}C(C{=}N_{dmgH\ or\ chgH})$ in (R/X)Co(dioximes)(dpgH)Py (dioxime = dmgH, chgH) (Supporting Information). This means the field effect is much higher in **1b**−**8b** as compared to that in similar mixed dioxime complexes with dmgH/dpgH and chgH/dpgH combinations.

The cis influence of the axial group (R or X) on dioxime ligands is monitored by $\Delta\delta^{13}C(C{=}N_{gH})$ and $\Delta\delta^{1}H(gH)$ in **1b**−**4b** with **5b**−**14b.** The values are consistently downfield in **1b**−**4b**, due to the larger anisotropy of X.

The ring current in the metallabicycle in cobaloximes results from 12 π delocalized electrons (8 electrons from $C{=}N_{dioxime}$ and 4 from cobalt). A good correlation, found previously, between $\Delta\delta^{13}C(C{=}N)$ and $\Delta\delta^{1}H(Py_\alpha)$ in $RCo(dioxime)_2B$ (dioxime = dmgH, chgH, dpgH, gH, mestgH; R = alkyl) suggests the presence of ring current throughout the Co(dioxime)$_2$ metallabicycle.[5a,8a,b,7] Thus, the electronic effect of one dioxime wing should transmit to the other wing in the present systems. This is seen when we compare the chemical shift $\delta^{13}C(C{=}N_{gH})$ in **1b**−**8b** with the corresponding value in $(R/X)Co(gH)_2Py$ or $(R/X)Co(dpgH)_2Py$ complexes (Supporting Information).

The chemical shifts of Py_α is affected not only by the trans effect of the R/X group but also by the ring current in the dioxime, as recently observed in $(R/X)Co(dioxime)_2Py$ complexes.[5a,7,8a] The coordination shift $\Delta\delta^{1}H(Py_\alpha)$ is −0.2 ppm in **1b**−**4b** and +0.2 ppm in **5b**−**14b**. This is due to the trans effect that works differently in inorganic and organic cobaloximes.[7,8] $\Delta\delta^{1}H(Py_\alpha)$ is exactly half of the corresponding values in either $(R/X)Co(gH)_2Py$ or $(R/X)Co(dpgH)_2Py$ complexes. This indicates a reduced ring current in the metallabicycle in **1b**−**15b**. The following correlations in **1b**−**8b** suggest complete de-

(18) Instead of $\delta^{13}C(C{=}N)$, the $\Delta\delta^{13}C(C{=}N)$ value has been taken. This is to avoid the direct effect of the substituent on the $\delta(C{=}N)$ value. $\Delta\delta^{13}C(C{=}N)$ represents the field effect (combined effect of cobalt anisotropy and ring current) and is equal to $\delta_{complex} - \delta_{free\ ligand}$.

localization leading to ring current in the metallabicycle, hence supporting our model:

$$\delta^1\mathrm{H(gH)} = 7.57(1) - 0.54(3)\ (\Delta\delta^1\mathrm{H(Py_\alpha)});\quad r^2 = 0.98,\ \mathrm{esd} = 0.01\ \mathrm{ppm}$$

$$\delta^{13}\mathrm{C(C{=}N_{gH})} = 139.23(8) - 7.46(50)\ (\Delta\delta^1\mathrm{H(Py_\alpha)});\quad r^2 = 0.97,\ \mathrm{esd} = 0.24\ \mathrm{ppm}$$

$$\delta^{13}\mathrm{C(C{=}N_{dpgH})} = 152.91(6) - 8.56(38)\ (\Delta\delta^1\mathrm{H(Py_\alpha)});\quad r^2 = 0.99,\ \mathrm{esd} = 0.18\ \mathrm{ppm}$$

$$\Delta\delta^{13}\mathrm{C(C{=}N_{dpgH})} = 4.62(1.7) + 1.14(0.3)\ (\Delta\delta^{13}\mathrm{C(C{=}N_{gH})});\quad r^2 = 0.99,\ \mathrm{esd} = 0.10\ (\mathbf{1b}-\mathbf{15b})$$

Since the chemical shift of the axial Co−C_α proton depends on the ring current in the dioxime moiety, $\delta(C_\alpha)$ in **1b**−**15b** should appear between the values in the parent complexes. This is what is observed also. Overall, the order follows dmestgH ≈ dpgH > gH-dpgH > dmgH-dpgH ≈ chgH-dpgH > gH > dmgH ≈ chgH. The mixed ligand complexes fit very well into the order and hence support the previous results on the (alkyl)Co(dioxime)$_2$Py complexes.[7,8a,9a] The order cannot be reached on the basis of ^{13}C values, since C_α is not observed in some cases.

Interestingly, $\delta^{13}C(C_\alpha)$ in **5b**−**7b** is drastically different and appears about 5−6 ppm upfield as compared to those values in **8b**−**14b**. This is because C_α in **12b** has higher "s" character than **6b**; the bond angles Co−C22−C23, observed in the X-ray structures, are 125.6 and 119.1° in **12b** and **6b**.

The Py_α proton is close to O−H···O and gets affected by the strength of this bond; the stronger the hydrogen bond, the more upfield the Py_α resonance: for MeCo(gH)$_2$Py, Py_α 8.61 ppm and O−H···O 17.74 ppm; for MeCo(gH)(dpgH)Py, Py_α 8.77 ppm and O−H···O 18.33 ppm; for MeCo(dpgH)$_2$Py, Py_α 9.00 ppm and O−H···O 18.90 ppm.

(c) UV−Vis Spectra. The complexes **5b**−**14b** show a Co−C CT band between 455 and 465 nm with intensity (log ϵ) in the range 3.00−3.60 and a MLCT band at 235−237 nm (log ϵ 4.50) (Table 2), whereas **1b**−**4b** show only the MLCT band in the range 245−260 nm (log ϵ 3.50−3.80). With pyridine being constant, the Co → C CT band depends on the cis influence of the dioxime. Unlike the previously studied systems RCo(dioxime)$_2$Py, two Co→dioxime MLCT transitions are expected in the mixed dioxime complexes. However, a broad band is observed, due to the overlap of two peaks. A good correlation is found between λ_{max}(MLCT) and ^{1}H and ^{13}C NMR coordination shifts:

$$\lambda_{max}(\mathrm{MLCT}) = 245.58(1.3) - 53.44(8.0)\ (\Delta\delta^1\mathrm{H(Py_\alpha)});\quad r^2 = 0.89,\ \mathrm{esd} = 3.8$$

$$\lambda_{max}(\mathrm{MLCT}) = 260.15(2.6) + 6.23(0.90)\ (\Delta\delta^{13}\mathrm{C(C{=}N_{dpgH})});\ r^2 = 0.89,\ \mathrm{esd} = 3.7$$

$$\lambda_{max}(\mathrm{MLCT}) = 288.72(7.0) + 7.04(1.0)\ (\Delta\delta^{13}\mathrm{C(C{=}N_{gH})});\quad r^2 = 0.87,\ \mathrm{esd} = 3.9$$

Cyclic Voltammetry. In the cyclic voltammogram of any cobaloxime, e.g. (R/X)Co(dioxime)$_2$Py, we expect three redox couples: Co(III)/Co(II), Co(II)/Co(I), and Co(IV)/Co(III). There is a lack of information on these three redox systems, as very little work has been reported on CV studies of cobaloximes. In particular, mixed ligand cobaloximes have never been studied before. The cyclic voltammograms of **1b** and **5b** along with the CV data of the parent cobaloximes ClCo(gH)$_2$Py and ClCo(dpgH)$_2$Py is given in Figures 1 and 2 and Tables 5 and 6.

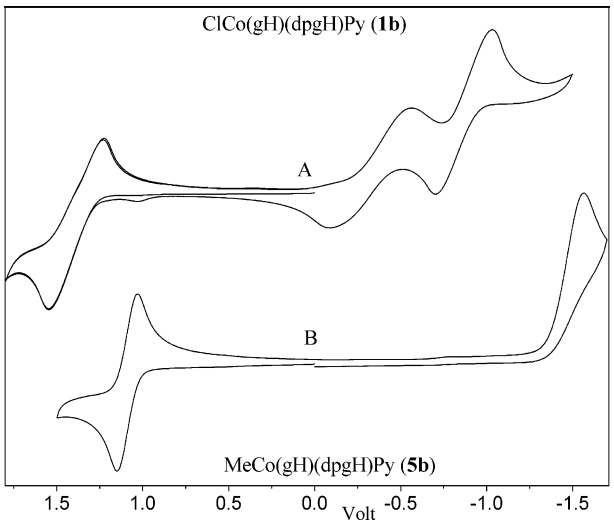

Figure 1. Cyclic voltammograms of **1b** (A) and **5b** (B) in CH_2Cl_2 with 0.1 M (TBA)PF_6 as supporting electrolyte at 0.2 V s^{-1} at 25 °C.

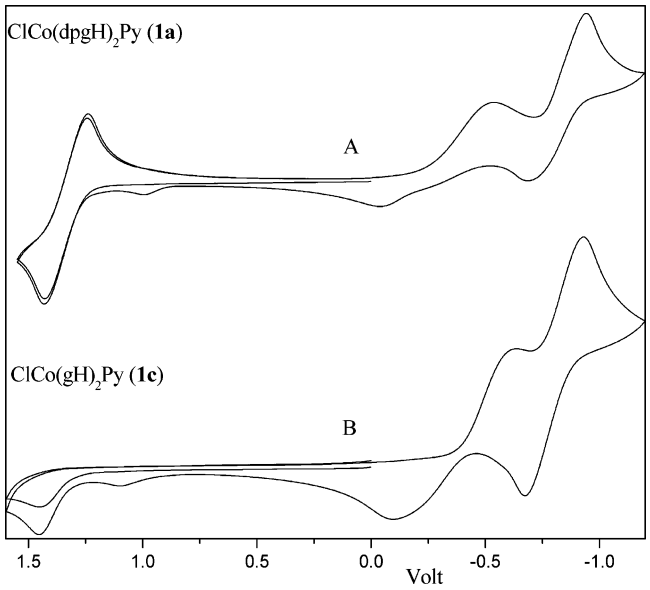

Figure 2. Cyclic voltammograms of **1a** (A) and **1c** (B) in CH_2Cl_2 with 0.1 M (TBA)PF_6 as supporting electrolyte at 0.2 V s^{-1} at 25 °C.

The cyclic voltammogram of **1b** (Figure 1A) shows two quasi-reversible redox couple in the reductive half at −0.33 and −0.87 V corresponding to Co(III)/Co(II) and Co(II)/Co(I), respectively. A comparison of these values with the CV data in the parent cobaloximes (Table 6) shows that Co^I(gH)(dpgH) is the strongest nucleophile among the three, and in the oxidation half one quasi-reversible wave corresponding to Co(IV)/Co(III) is observed and the value lies (+1.39 V) between those of the parent cobaloximes.

In contrast, **5b** (Figure 1B) shows a different behavior; only one completely irreversible reductive half corresponding to Co(III)/Co(I) (from i_{pc}) at −1.57 V is obtained. The reduction, as expected, is much easier in **1b** as compared to **5b** due to the

Table 5. CV Data for 1b and 5b in Dichloromethane and (TBA)PF_6 at 0.2 V s^{-1} and 25 °C

	Co(III)/Co(II)					Co(II)/Co(I)					Co(IV)/Co(III)				
no.	$E_{1/2}$ (V)[a] (ΔE_p (mV))	$E_{1/2}$ (V)[b]	i_{pc} (μA)	i_{pa} (μA)	i_{pa}/i_{pc}	$E_{1/2}$ (V)[a] (ΔE_p (mV))	$E_{1/2}$ (V)[b]	i_{pc} (μA)	i_{pa} (μA)	i_{pa}/i_{pc}	$E_{1/2}$ (V)[a] (ΔE_p (mV))	$E_{1/2}$ (V)[b]	i_{pc} (μA)	i_{pa} (μA)	i_{pa}/i_{pc}
1b	−0.33 (470)	−0.84	28.0	28.0	1.0	−0.87 (320)	−1.38	40	41	1.03	1.39 (290)	0.88	43	51	1.19
5b						−1.57[c]	−2.08	18			1.09 (120)	0.58	9.8	10.2	1.04

[a] Vs Ag/AgCl. [b] Vs Fc/Fc^+. [c] Value refers to E_{pc}.

Table 6. CV Data for $ClCo(dpgH)_2Py$, ClCo(gH)(dpgH)Py, and $ClCo(gH)_2Py$ in CH_2Cl_2 and (TBA)PF_6 at 0.2 Vs^{-1} at 25 °C

	Co(III)/Co(II)		Co(II)/Co(I)		Co(IV)/Co(III)	
	$E_{1/2}$ (V)[a] (ΔE_p (mV))	$E_{1/2}$ (V)[b]	$E_{1/2}$ (V)[a] (ΔE_p (mV))	$E_{1/2}$ (V)[b]	$E_{1/2}$ (V)[a] (ΔE_p (mV))	$E_{1/2}$ (V)[b]
$ClCo(dpgH)_2Py$	−0.29 (490)	−0.80	−0.82 (260)	−1.33	1.33 (150)	0.82
ClCo(gH)(dpgH)Py	−0.33 (470)	−0.84	−0.87 (320)	−1.38	1.39 (290)	0.88
$ClCo(gH)_2Py$	−0.36 (420)	−0.87	−0.80 (250)	−1.31	1.45[c]	0.94

[a] Vs Ag/AgCl. [b] Vs Fc/Fc^+. [c] Value refers to E_{pa}.

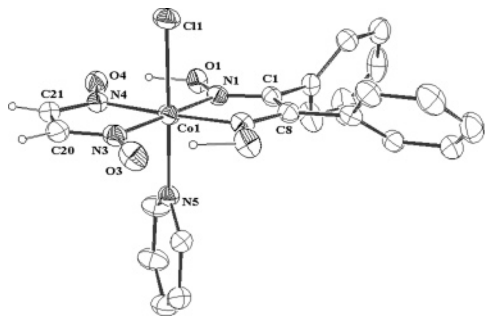

Figure 3. Ortep diagram of ClCo(gH)(dpgH)Py (**1b**).

higher cobalt anisotropy in **1b**. The oxidative half shows one reversible couple corresponding to Co(IV)/Co(III) at +1.09 V.

The CV data for both the reductive and the oxidative half in **1b** has been rationalized on the basis of the cobalt anisotropy. From ab initio calculations on **1b**, the HOMO, responsible for the oxidation potential, is based only on the equatorial ligand and has the total contribution of both gH and dpgH orbitals. However, the LUMO, which is responsible for the reduction potential, results from the combination of all the ligand orbitals and metal d orbitals (Supporting Information). This means that the oxidation half is mainly controlled by the charge density on the dioxime moiety which is related to cobalt anisotropy and thus arises only from the $Co(dioxime)_2^+$ metallabicycle. The reduction half depends on both axial and equatorial ligands.

X-ray Crystallographic Studies. The “Ortep3” diagrams of the molecular structures of **1b**, **6b**, and **12b** along with selected numbering schemes are shown in Figures 3−5, respectively. Selected bond lengths, bond angles, and structural parameters are given in Table 7. The crystal structure of **6b** contains two molecules in its asymmetric unit. Since there is a structural variation, they are numbered as **6b-I** and **6b-II** and the crystal data are given separately (Table 7).[19] The geometry around the central cobalt atom is distorted octahedral. The cobalt atom is linked to four nitrogen atoms, two each from the dpgH and gH ligands in the equatorial plane, and the axial positions are occupied by R/X and pyridine. The cobalt atom deviates 0.022 Å from the mean equatorial CoN_4 plane toward the neutral pyridine ligand in **1b**, while the deviations are −0.0326, 0.0128, and 0.0383 Å in **6b-I**, **6b-II**, and **12b**, respectively. A negative sign means that the deviation is toward the axial R group.

(19) Steed, J. W. *CrystEngComm* **2003**, *5*, 169.

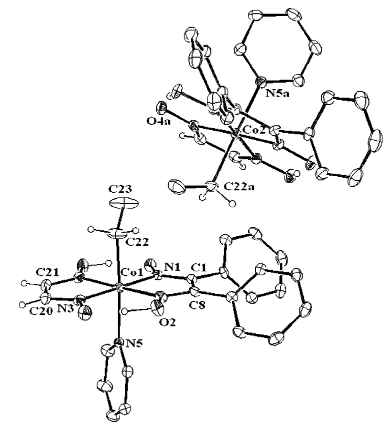

Figure 4. Ortep diagram of EtCo(gH)(dpgH)Py (**6b-I** and **6b-II**; two molecules in the asymmetric unit).

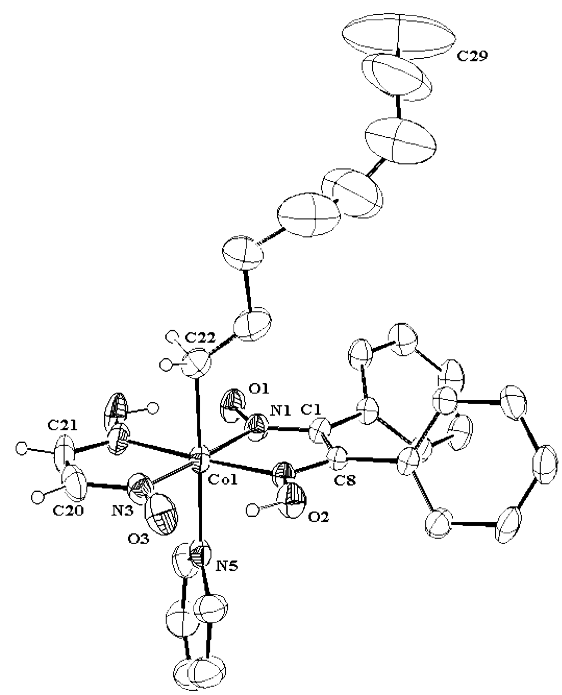

Figure 5. Ortep diagram of (octyl)Co(gH)(dpgH)Py (**12b**).

The pyridine ring is almost parallel to the dioxime C−C bonds, with its conformation being defined by twist angles[20a] of 86.08, 88.80, 73.68, and 88.88° in **1b**, **6b-I**, **6b-II**, and **12b**, respectively. The butterfly bending angle[20b] α in **1b** is 2.81°,

Table 7. Selected Bond Lengths and Bond Angles

param	1b	6b		12b
		6b-I	6b-II	
Co−Cl (Å)	2.2410(8)			
Co−C22 (Å)		2.022(2)	2.018(2)	2.028(7)
Co−N5 (Å)	1.966(2)	2.0619(18)	2.0720(17)	2.066(5)
Co−N1 (Å)	1.888(2)	1.8791(17)	1.8759(18)	1.881(5)
Co−N2 (Å)	1.888(2)	1.8854(17)	1.8766(17)	1.869(4)
Co−N3 (Å)	1.910(2)	1.8851(18)	1.8855(18)	1.886(5)
Co−N4 (Å)	1.905(2)	1.8959(17)	1.8833(17)	1.891(5)
C1−C8 (Å)	1.481(4)	1.473(3)	1.474(3)	1.474(7)
C21−C20 (Å)	1.442(5)	1.445(3)	1.444(3)	1.414(10)
C═N (dpgH wing) (Å)	1.304(3)	1.302(3)	1.302(3)	1.305(7)
	1.305(3)	1.309(3)	1.312(3)	1.296(7)
C═N (gH wing) (Å)	1.296(4)	1.291(3)	1.293(3)	1.313(8)
	1.296(4)	1.300(3)	1.293(3)	1.296(8)
N5−Co−Cl (deg)	178.82(7)			
N5−Co−C22 (deg)		177.48(8)	176.18(9)	178.1(3)
Co−C22−C23 (deg)		117.64(15)	119.09(19)	125.6(6)
d	0.022	−0.0326	0.0128	0.0383
α[a] (deg)	2.81	0.93	5.03	0.85
τ[b] (deg)	86.08	88.80	73.68	88.88

[a] Butterfly bending angle. [b] Twist angle of pyridine with respect to the line joining the midpoints of C1−C8 and C20−C21.

while they are 0.93, 5.03, and 0.85° in **6b-I**, **6b-II**, and **12b**, respectively.

The Co−N5 bond distance in **1b** is shorter than in **6b-I**, **6b-II**, and **12b**, indicating a lower trans effect of chloride as compared to that of the alkyl group. The equatorial moiety affects the Co−Cl bond distance: for example, the Co−Cl bond distance in **1b** is longer than the corresponding value in ClCo(dpgH)(dioxime)Py (dioxime = dmgH, chgH).[9a] This is due to the cobalt anisotropy in gH being lower than in dmgH, chgH, or dpgH. It has been shown before that the inorganic and organic cobaloximes behave differently, since the Co → dioxime back-donation is effected by the axial ligands.[7] Hence the Co−N_{eq} bond lengths are shorter in the dpgH wing (∼0.02 Å) as compared to those in the gH, dmgH, or chgH wing in **1b** or in the corresponding inorganic cobaloximes,[9a] whereas these are similar in the organocobaloximes.

There are no significant differences in Co−C and Co−N5 bond lengths from those in the other analogous organocobaloximes. The Co−C−C bond angle is exceptionally higher (125.6°) in **12b** as compared to those in **6b-I** and **6b-II**, indicating a higher "s" character.[21] This is why the ^{13}C NMR chemical shift of Co−CH_2 is 5−6 ppm downfield in **8b**−**14b** from those in **5b**−**7b**.

There are some significant differences in the structures of **6b-I** and **6b-II**. In general, the orientation of the Co−A−B bond in any (R/X)Co(dioxime)$_2$Py compound lies above one of the dioxime units. This is what is observed in **6b-I.** However, in **6b-II** this bond lies above the O−H···O unit, thus causing distortion in the values of α, τ, and *d*. We think that the change in orientation in **6b-II** is due to nothing but the crystal packing.

Supramolecular chemistry exploits noncovalent interactions to assemble large superstructures from molecular subunits in a rapid and reversible way. Since these processes occur under thermodynamic control, many of these superstructures are not very stable, particularly in solution. The possibility of constructing molecular architectures linked by covalent bonds under thermodynamic control (dynamic covalent chemistry) is therefore extremely appealing. In the crystal structures of **1b, 6b**, and **12b** the interplay of weak interactions that lead to supramolecules are C−H···π (Ph or Py), C−H···O, and π···π stacking. The metric parameters for these weak interactions are given in Table 8.

Table 8. Metric Parameters of C−H···O and C−H···π Interactions for 1b, 6b, and 12b[a]

bond	distance (Å) H····A	distance (Å) D····A	angle (deg) D−H····A
Compound **1b**			
C−H···O			
C18−H18···O1	2.539	3.152	125.79
C3−H3···O4	2.693	3.327	126.03
C4−H4···O4	2.983	3.496	119.93
C6−H6···O1	2.749	3.758	159.81
C20−H20···O2	2.799	3.739	153.08
C−H···π			
C20−H20···π center (C9−C14)	2.845	3.362	111.85
C11−H11···π center (Py ring)	3.002	3.737	133.85
C17−H17···π center (C9−C14)	2.893	3.666	141.99
Compound **6b**			
C14a−H14a···O3	2.558	3.339	139.49
C7−H7···O2a	2.744	3.569	145.57
C14−H14···O3a	2.776	3.496	133.30
C13−H13···O1	2.644	3.480	147.03
C17−H17···O1	2.568	3.367	141.11
C6a−H6a···O4a	2.442	3.344	158.56
C3a−H3a···O4a	2.569	3.244	128.29
C13a−H13a···O4	2.712	3.403	130.20
Compound **12b**			
C11−H11···O3	2.684	3.419	136.55
C12−H12···O4	2.551	3.400	151.93
C28−H28b···O3	2.738	3.560	143.46
C11−H11···O3	2.885	3.686	140.39

[a] Abbreviations: D = donor atom, A = acceptor atom.

1b forms a 2-D helical structure due to hydrophobic C−H···π interactions, an observation made for the first time in cobaloximes. The helix topology is a current target in crystal engineering strategy.[11b,22] A right-handed helix present in the crystal structure is shown in Figure 6a. The helix is formed through two C−H···π interactions (C20−H20···phenyl ring π center and C11−H11···Py ring π center) along the 2_1 screw axis (Figure 6b). Each coil of the helix contains two cobaloxime residues, and the distance between the coils is 10.672(1) Å. Furthermore, this helical structure is connected to another helix and forms a two-dimensional network through a C−H···π bond (C17−H17···phenyl ring π center).

Another interesting aspect of the structure of **1b** is that it forms a pillared[23] three-dimensional lamellar network due to five intermolecular C−H···O hydrogen-bonding interactions. Intermolecular contacts of the C−H···O type with H···O distances of 2.0−3.1 Å and C−H···O angles of 110−180° are within accepted ranges.[12a,22a] The extended structure in **1b** may be understood by analyzing it in a stepwise manner. A lamellar structure (Supporting Information) is formed due to four

(20) (a) The dihedral angle between the plane of pyridine and the plane containing a line joining the midpoints of C1−C8 and C20−C21. (b) The dihedral angle between the equatorial halves (O1N1C1C2N2O2 plane and O3N3C20C21N4O4 plane).

(21) Starr, E. J.; Bourne, S. A.; Caira, M. R.; Moss, J. R. *J. Organomet. Chem.* **1995**, *490*, C20.

(22) (a) Vishweshwar, P.; Thaimattam, R.; Jaskolski, M.; Desiraju, G. R. *Chem. Commun.* **2002**, 1830. (b) Coupar, P. I.; Glidewell, C.; Ferguson, G. *Acta Crystallogr., Sect. B* **1997**, *53*, 521. (c) Piguet, C.; Bermardinelli, G.; Hopfgartner, G. *Chem. Rev.* **1997**, *97*, 2005. (d) Katz, T. J. *Angew. Chem., Int. Ed.* **2000**, *39*, 1921. (e) Vazquez, M.; Taglietti, A.; Gatteschi, D.; Sorace, L.; Sangregorio, C.; Gonzalez, M.; Maneiro, M.; Pedrido, R. M.; Bermejo, M. R. *Chem. Commun.* **2003**, 1840. (f) Rowan, A. E.; Nolte, R. J. M. *Angew. Chem., Int. Ed.* **1998**, *37*, 63. (g) Geib, S. J.; Vicent, C.; Fan, E.; Hamilton, A. D. *Angew. Chem., Int. Ed. Engl*. **1993**, *32*, 119.

(23) (a) Holman, K. T.; Pivovar, A. M.; Swift, J. A.; Ward, M. D. *Acc. Chem. Res.* **2001**, *34*, 107. (b) Clearfield, A.; Wang, Z. *Dalton Trans.* **2002**, 2937.

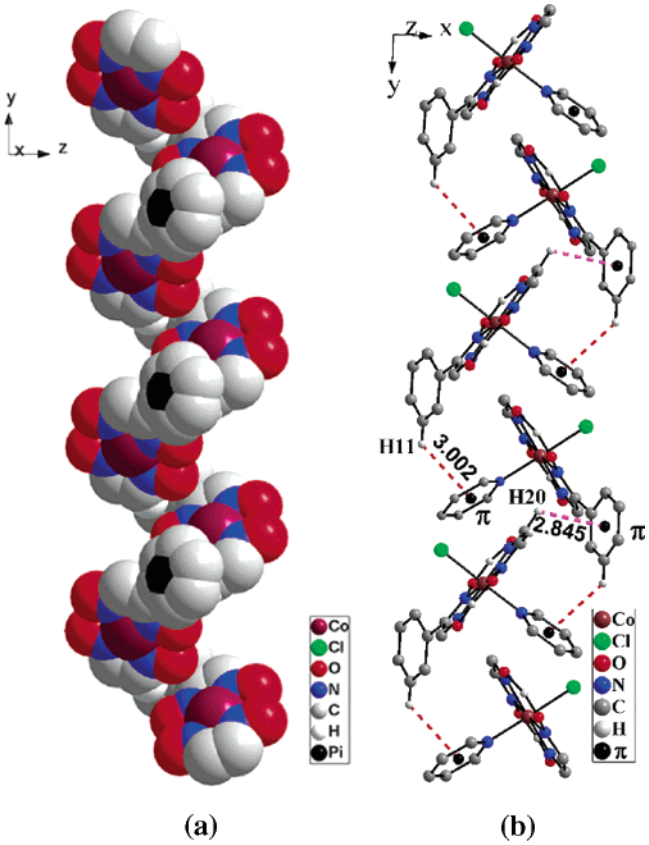

Figure 6. (a) Space-filling view of the right-handed helix of **1b**. (b) 1-D helical assembly of **1b** along the *y* axis. One of the phenyl rings and all of the hydrogen atoms, except those involved in hydrogen bonding, have been omitted for clarity.

C−H···O hydrogen bonds (C18−H18···O1, C3−H3···O4, C4−H4···O4, and C20−H20···O2). This leads to a nearly planar sheet that acts as floors and ceilings (the neighboring Co−Co distance is 10.673(1) Å; a channel with height and width of ~3.131(5) × 13.040(4) Å^2, respectively, is formed). The lamellar structure thus formed is taken into the third dimension by one more C−H···O hydrogen bond (C6−H6···O1) that acts as a pillar (Figure 7). The average interlayer separation (distance between two cobalt atoms in adjacent layers) is 10.612(1) Å. The width between the pillars in a given row is 13.132(6) Å. Thus, a 1-D channel is formed with dimensions of about 10 × 13 Å^2. The major portion of the cavity has been occupied by one of the phenyl rings of the dpgH ligand, which is not shown for clarity.

The crystal-packing diagram of **6b** shows $\pi\cdots\pi$ stacking (Figure 8).[24] The distance between the centroids of stacked pyridine rings is 3.917 Å, and the closest C−C bond is 3.900 Å. Crystal-packing diagrams of **6b-I** and **6b-II** also show the presence of extensive intermolecular C−H···O interactions leading to the formation of a three-dimensional network containing a series of rings (Supporting Information). There are three C−H···O interactions (C14a−H14···O3, C7−H7···O2a, and C14−H14···O3a) between **6b-I** and **6b-II**.

The crystal-packing diagram of compound **12b** shows a two-dimensional lamellar network involving four intermolecular C−H···O contacts. A one-dimensional double-chain polymeric network is formed due to two C−H···O hydrogen bonds (C5−H5···O4 and C4−H4···O3). Two such 1-D double chains are

(24) (a) Janiak, C. *Dalton Trans.* **2000**, 3885. (b) Okawa, H. *Coord. Chem. Rev.* **1988**, *92*, 1.

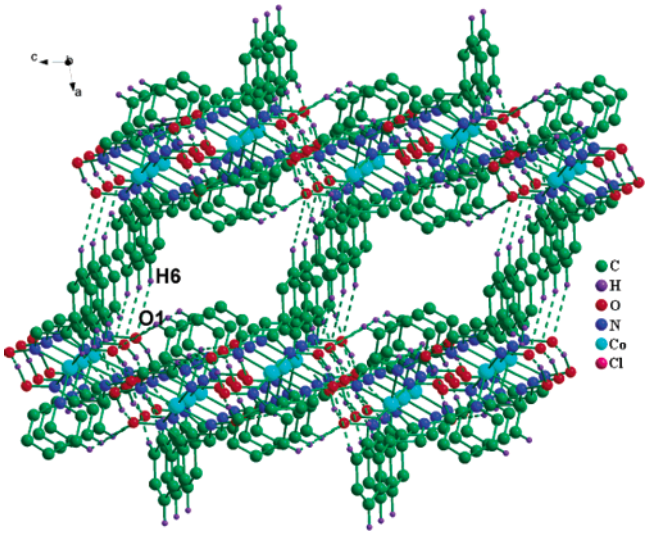

Figure 7. 3-D pillared network of **1b** along the *b* axis. The Cl atom, one of the phenyl groups, and most of the hydrogen atoms have been omitted for clarity.

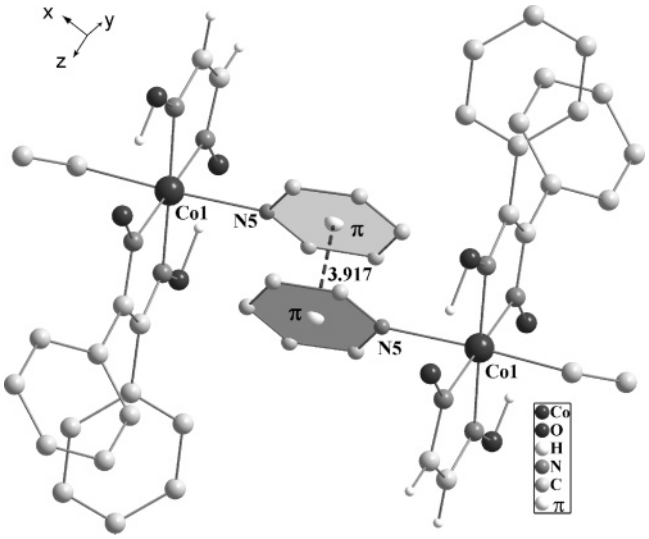

Figure 8. $\pi\cdots\pi$ stacking in **6b-II**.

connected through two more C−H···O hydrogen bonds (C27−H27···O2 and C28−H28···O2) to form a 2-D lamellar network (the neighboring Co−Co distance is 12.304(10) Å; a channel with width and height of ~8.772(270) × 8.543(267) Å^2, respectively (Supporting Information)). An interesting aspect of this 2-D lamellar network is that it forms a hydrophobic channel due to the long alkyl chain. The crystal packing of **12b** resembles the crystal packing of *n*-$C_{14}H_{29}Co(dmgH)_2Py$.[21] However, in the latter the packing was determined chiefly by van der Waals forces and no intermolecular hydrogen bonds were detected. This sort of arrangement is reminiscent of surfactant molecules.

Conclusion. The spectral data are interrelated, and a good correlation is found between $\Delta\delta^1H(Py_\alpha)$ with $\delta^1H(gH)$, $\delta^{13}C(C{=}N_{gH})$ and $\delta^{13}C(C{=}N_{dpgH})$, indicating the ring current throughout the $Co(dioxime)_2^+$ metallabicyle. Similarly, λ_{max}(MLCT) correlates well with $\Delta\delta^1H(Py_\alpha)$, $\delta^{13}C(C{=}N_{gH})$ and $\delta^{13}C(C{=}N_{dpgH})$. These correlations are understood much better when both ring current and cobalt anisotropy are considered to operate together (field effect), a model proposed recently by us. The overall cis influence order for the dioximes is found to be dmestgH > dpgH > gH-dpgH > dmgH-dpgH > chgH-dpgH > dmgH > gH >

chgH. The CV data also show that there is a mixing of two dioxime ligands, and the data have been rationalized on the basis of the cobalt anisotropy. The X-ray structure and crystal packing in ClCo(gH)(dpgH)Py, C_2H_5Co(gH)(dpgH)Py, and C_8H_{17}Co(gH)(dpgH)Py exhibit some weak supramolecular interactions to form a two- or three-dimensional array such as helix, pillared, and lamellar networks. ClCo(gH)(dpgH)Py shows a right-handed helix.

Acknowledgment. We thank the DST (Grant No. SR/S1/IC-12/2004) New Delhi, India, for financial support.

Supporting Information Available: An MO picture of ab initio calculations and additional figures, figures detailing the $^{1}H-^{13}C$ correlation experiments, tables containing coordination shift data and effects of one wing on the other wing, and CIF files giving crystallographic data for **1b**, **6b**, and **12b**. This material is available free of charge via the Internet at http://pubs.acs.org. Crystallographic data have also been deposited with the Cambridge Crystallographic Data Center, and CCDC numbers for the structures of **1b**, **6b**, and **12b** are 212320, 265405, and 265404, respectively.

OM050919X